Simultaneous noncontact AFM and STM of Ag:Si(111)-($\sqrt{3} \times \sqrt{3}$)R30°

Adam Sweetman,[1] Andrew Stannard,[1] Yoshiaki Sugimoto,[2] Masayuki Abe,[3] Seizo Morita,[2] and Philip Moriarty[1]

[1]*School of Physics and Astronomy, University of Nottingham, Nottingham NG7 2RD, United Kingdom*
[2]*Graduate School of Engineering, Osaka University, 2-1 Yamada-Oka, Suita, Osaka 565-0871, Japan*
[3]*Graduate School of Engineering, Nagoya University, Furo-cho, Chikusa-ku, Nagoya 464-8603, Japan*

The Ag:Si(111)-($\sqrt{3} \times \sqrt{3}$)R30° surface structure has attracted considerable debate concerning interpretation of scanning tunneling microscope (STM) and noncontact atomic force microscope (NC-AFM) images. In particular, the accepted interpretation of atomic resolution images in NC-AFM has been questioned by theoretical and STM studies. In this paper, we use combined NC-AFM and STM to conclusively show that the inequivalent trimer (IET) configuration best describes the surface ground state. Thermal-averaging effects result in a honeycomb-chained-trimer (HCT) appearance at room temperature, in contrast to studies suggesting that the IET configuration remains stable at higher temperatures [Zhang, Gustafsson, and Johansson, Phys. Rev. B **74**, 201304(R) (2006) and J. Phys.: Conf. Ser. **61**, 1336 (2007)]. We also comment on results obtained at an intermediate temperature that suggest an intriguing difference between the imaging mechanisms of NC-AFM and STM on structurally fluctuating samples.

I. INTRODUCTION

The Ag:Si(111)-($\sqrt{3} \times \sqrt{3}$)R30° surface reconstruction [Ag:Si(111) hereafter] has undergone intensive investigation by a plethora of surface science techniques,[1] in part due to the considerable interest in metal-semiconductor interfaces. Despite this range of studies, interpretation of images of the Ag:Si(111) surface produced by scanning probe microscopes (SPM) has been a topic of considerable debate. After initial STM and theoretical investigations,[1–8] it was widely accepted that the HCT configuration best described the surface reconstruction.[1] In the HCT configuration, Si adatoms form covalently bound Si trimers; each of these Si adatoms are terminated by an Ag atom. Further to this, these Ag atoms associate into Ag trimers; each Ag atom links two Ag trimers, resulting in a chained honeycomb arrangement of Ag trimers, see Fig. 1(a). Subsequent studies suggested that the surface undergoes a transition to an asymmetric IET configuration at low temperatures.[11,12] In the IET configuration, a 6° rotation of Ag-Si bonds results in adjacent Ag trimers becoming inequivalent in size. Since this rotation can occur in two directions, two asymmetric ground states of opposite chirality (referred to as IETa and IETb) are possible, see Figs. 1(b) and 1(c). These two chiral configurations are separated by a small energy barrier of order 100 meV per unit cell.[13]

More recently, it was suggested that the IET configuration was also observable at room temperature and that previous observations of an HCT appearance were the result of particular tip states and choice of tunneling parameters.[9,10] This was in contrast to the accepted interpretation of the HCT appearance being a thermal average of oscillations between the two IET chiralities and that observed asymmetries at room temperature could be assigned to tip asymmetries.[7] In particular, doubt was cast over the interpretation of NC-AFM images acquired at room temperature,[14,15] suggesting that images with Ag-atom contrast could be interpreted as an "all inclusive" imaging mode that produced topographic maxima over the centers of both Ag and Si trimers, similar to that observed in some STM studies.[9,10] However, this study did not elaborate as to why the IET configuration might be stable at room temperature,

when similar bistable systems with *larger* energy barriers, for example Si(100) (with a barrier for dimer flipping of order 200–400 meV),[16–18,31] have been shown to oscillate at room temperature, resulting in time-averaged appearances.

Nonetheless, an important qualification in the comparison between the theoretically calculated barrier for Ag:Si and Si(100) is that often the Si(100) barrier is given for flipping a *single* dimer, whereas the Ag:Si calculations assume that all of the trimers on the surface change *simultaneously*. In practice, the energy barrier for a single trimer to change configuration will be higher, as, if the surrounding environment does not change, it will be forced into a highly strained configuration. However, it is difficult to state the exact degree of underestimation, as forcing a single trimer to change may result in a "domino" effect in the surrounding trimers resulting in a large scale portion of the surface changing as the result of a single trimer being modified. Consequently, any calculation attempting to determine realistic barriers for a single trimer to change will intrinsically have to take into account long-range effects, and is likely to be extremely computationally expensive. Nonetheless, it seems unlikely that any underestimation would raise the barrier sufficiently to ensure stability at room temperature. In this study, all Ag:Si(111) images are compared to the particular HCT and IET models proposed by Aizawa *et al.*[11]

Although the HCT structure observed at room temperature is generally understood to be a "HCT-like" appearance, resulting from the thermal fluctuation between the two IET configurations faster than the sample rate of the feedback loop, some studies have, however, suggested that a "true" HCT phase occurs at room temperature.[32] We note that the room temperature experiments presented in this paper will not distinguish between an HCT and HCT-like appearance, and are mainly concerned with identifying whether the IET structure is observable at room temperature. Nonetheless, the interpretation of the data in the discussion assumes the HCT structure at room temperature is most likely an HCT-like appearance resulting from the thermal fluctuation of the IET structure.
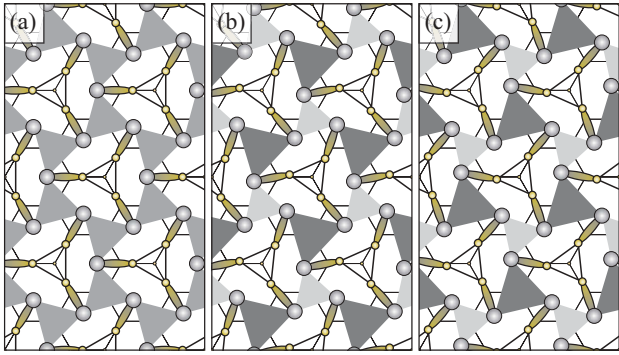
FIG. 1. (Color online) Top-down views of the (a) HCT, (b) IETa, and (c) IETb models of the Ag:Si(111) surface.[11] Key: large (small) circles, Ag (Si) atoms; ellipses, Ag-Si bonds; light (dark) triangles, small (large) Ag trimers.

On the Ag:Si(111) surface, it is generally accepted that during STM imaging of empty states, topographic maxima appear over the Ag trimer centers and the Si trimers are not imaged.[1,7,8,19,20] In filled states, STM can either show the Ag trimer centers, or occasionally the Ag atom positions,[12] although this is tip and bias dependent. The Ag:Si(111) surface charge density has been shown to be localised over the Ag trimer centers[6,11] and greater over small Ag trimers in the IET configuration, which consequently appear both larger and brighter in STM compared to the large Ag trimers. Special tip states have resulted in an alternative imaging mode where both Ag and Si trimers are imaged simultaneously.[9] In contrast to STM images, NC-AFM images of Ag:Si(111) are somewhat poorly understood. Experimental studies at room temperature suggested two imaging modes: one that imaged the Ag atom positions (assigned to an Ag-terminated tip)[14] and another that showed set-point-dependent contrast relating to Ag-Si bonds (assigned to an Si-terminated tip).[15] A subsequent theoretical study suggested that with an Si-terminated tip the Ag atom positions should be imaged,[13,21–23] with a combination of tip-surface interaction and thermal effects resulting in an HCT appearance at room temperature due to oscillations between the two IET chiralities.

In this study, we use a combined NC-AFM/STM technique, at room and cryogenic temperatures, to conclusively show that while the IET configuration best describes the surface ground state, the surface has an HCT appearance at room temperature, most likely due to thermal fluctuations. We show that NC-AFM can resolve Ag atom positions in the IET configuration at low temperature and image boundaries between different IET chiralities. Importantly, we also demonstrate how changes in tip termination result in switches in observed contrast, and how simultaneous acquisition of NC-AFM and STM data can resolve long-standing issues regarding the interpretation of SPM images of the Ag:Si(111) surface. By cross-checking simultaneously acquired data, we show that the accepted interpretation of NC-AFM and STM images are self-consistent. Intriguingly, data acquired at an intermediate temperature show differences in contrast between the two channels, suggesting that the interplay of tip position and energy barriers at the surface, over the range of a cantilever oscillation cycle, may play an important role in interpreting data on structurally fluctuating surfaces.

II. EXPERIMENTAL DETAILS

Experiments were performed using two separate setups. Room-temperature measurements were carried out in the Osaka group's laboratories with a custom-built NC-AFM/STM, using commercial platinum-iridium-coated silicon cantilevers with large (∼14–20 nm) oscillation amplitudes. Cryogenic temperature experiments were performed in the Nottingham group's laboratories with a commercial (Omicron Nanotechnology GmbH) qPlus NC-AFM/STM in an LHe/LN$_2$ bath cryostat (sample temperature approximately 5 K with LHe cooling and 77 K with LN$_2$ cooling) using commercial qPlus sensors[24] (tungsten wire attached to the end of a quartz tuning fork) with oscillation amplitudes of ∼0.2 nm. Ag:Si(111) surfaces were prepared by producing a clean Si(111) surface by standard flashing/annealing, and subsequently depositing Ag whilst annealing the surface to ensure a good reconstruction and to remove excess Ag. All measurements were performed in constant frequency shift (Δf) feedback whilst maintaining a constant oscillation amplitude (a). In the text, all biases (V_{gap}) are stated as effective sample biases, but it should be noted that in the low-temperature experiments the bias was applied to the tip. Peak average tunnel current values ($\langle I_t \rangle_{max}$) are given where a simultaneous tunnel current was detected. When performing STM imaging, we often acquired images using constant tunnel current feedback with an oscillating tip. These are designated as dynamic STM (dSTM) images, and the tunnel current set points quoted in these cases are also the average tunnel current detected over the course of a oscillation cycle. Further experimental details are provided in the Supplemental Material.[33]

III. RESULTS

A. Imaging at room temperature (300 K)

Figure 2 shows representative NC-AFM topographs of the Ag:Si(111) surface taken at room temperature, alongside the corresponding simultaneously-acquired tunnel current data. In Fig. 2(a), topographic contrast related to Ag-Si bonds is observed, as previously reported.[15] This interpretation is confirmed by the tunnel current data, see Fig. 2(b), as assigning topographic maxima to Ag-Si bonds results in tunnel current maxima aligning to Ag trimer centers. In Fig. 2(c), the same surface is imaged with a different tip apex, resulting in topographic maxima over Ag atoms. Crucially, the tunnel current data also confirm this, see Fig. 2(d), as assigning topographic maxima to Ag atoms again results in tunnel current maxima located over the Ag trimer centers. Both the topographic and tunnel current data show an HCT appearance—there is no Ag trimer asymmetry in the topography or tunnel current channels.

In Fig. 2(e), the tip switches between contrast originating from Ag atoms to Ag-Si bonds. Importantly, the upper part of the topograph displays an HCT appearance of Ag atoms, whilst the tunnel current has an IET appearance, see Fig. 2(f). However, after the change in tip state to image Ag-Si-bond topography, the tunnel current shows no such asymmetry. Additionally, close inspection of the Ag-atom topography
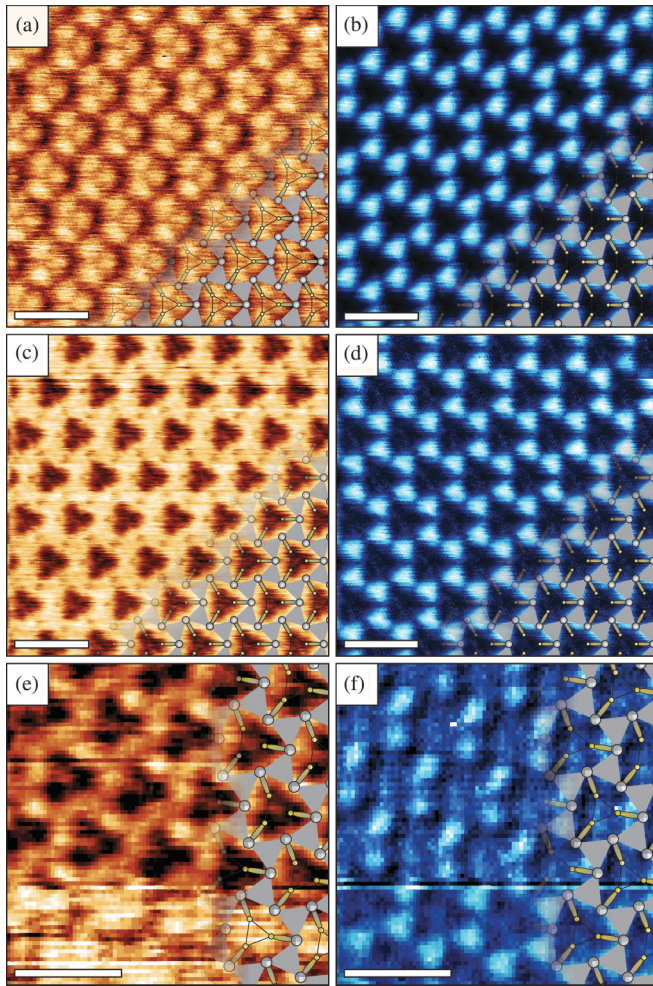
FIG. 2. (Color online) Topographic NC-AFM and simultaneously acquired tunnel current images taken at room temperature. (a) Topograph displaying Ag-Si-bond contrast and (b) the corresponding tunnel current image with the HCT model overlaid ($\Delta f = -60.9$ Hz, $a = 16.1$ nm, $V_{gap} = +500$ mV, $\langle I_t \rangle_{max} \simeq 7$ nA). (c) Topograph displaying Ag-atom contrast and (d) the corresponding tunnel current image ($\Delta f = -48.9$ Hz, $a = 17.3$ nm, $V_{gap} = -500$ mV, $\langle I_t \rangle_{max} \simeq 5$ nA). (e) Topograph exhibiting a spontaneous tip change and (f) the corresponding tunnel current image ($\Delta f = -59.2$ Hz, $a = 14.6$ nm, $V_{gap} = -500$ mV, $\langle I_t \rangle_{max} \simeq 300$ pA, a split scale has been used to enhance contrast with both tip states). Note that FFT filtering has been applied to (a) and (c) to remove mechanical noise. All scale bars are 1 nm.

reveals that one Ag atom of each Ag trimer appears slightly brighter, suggesting a small "double tip" may be influencing imaging [similar phenomena have been reported during simultaneous imaging of Si(111)-(7×7)].[25] Throughout all room-temperature experiments, using multiple cantilevers, all imaging that demonstrated simultaneous atomic resolution, in both the topography and tunnel current channels, displayed an HCT appearance in both modes. Consequently, we suggest that the IET appearance sometimes observed in tunnel current images at room temperature may be the result of tip artefacts, similar to those proposed theoretically.[7]

Importantly, even if the IET configuration were to be observable at room temperature in some circumstances (perhaps

due to pinning by defects) then in order to conclusively demonstrate this using scanning probe techniques, it would be necessary to image *both* IETa and IETb structures in the same scan (e.g., by imaging at a step edge, or phase boundary), as is readily done at low temperature (see next section). Without imaging both phases simultaneously it is difficult to distinguish conclusively between tip artifacts and the true surface structure.

B. Imaging at low temperature (5 K)

Although the NC-AFM data at room temperature shows an HCT appearance, an alternative explanation is possible. To achieve atomic resolution in NC-AFM, it is generally necessary to approach closer to the surface compared to STM.[25] Consequently, the observed HCT appearance may be the result of tip-induced surface perturbation. Therefore it is necessary to confirm that NC-AFM is indeed capable of imaging an unperturbed IET configuration. Figure 3 demonstrates this to be the case by showing data, acquired at 5 K, that unambiguously demonstrates NC-AFM observation of an IET configuration. Fig. 3(a) is an NC-AFM topograph, showing Ag-Si-bond contrast, acquired with a small bias applied. Figure 3(b) shows the corresponding tunnel current image, which displays a strikingly clear set of triangles centered on the Ag trimers. Figure 3(c) is acquired in the exact same region after a spontaneous tip change which results in Ag-atom contrast. The Ag atom positions in this instance correspond to those
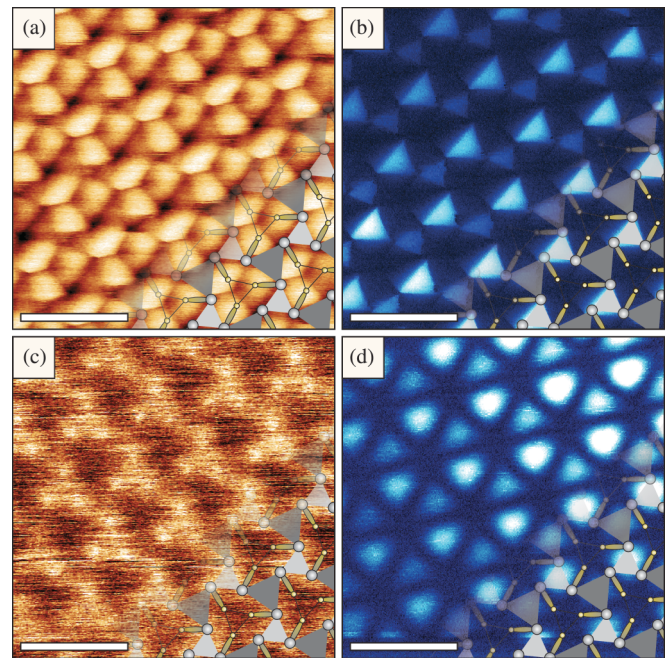
FIG. 3. (Color online) Topographic NC-AFM and simultaneously acquired tunnel current images, taken at 5 K, showing imaging of the exact same area before and after a spontaneous tip change, with the IETb model overlaid. (a) Topograph displaying Ag-Si-bond contrast and (b) the corresponding tunnel current image ($\Delta f = -63.0$ Hz, $a = 0.2$ nm, $V_{gap} = +150$ mV, $\langle I_t \rangle_{max} \simeq 22$ pA). (c) Topograph displaying Ag-atom contrast and (d) the corresponding tunnel current image ($\Delta f = -67.1$ Hz, $a = 0.2$ nm, $V_{gap} = +170$ mV, $\langle I_t \rangle_{max} \simeq 32$ pA). See Supplemental Material for the corresponding zero-bias images. All scale bars are 1 nm.
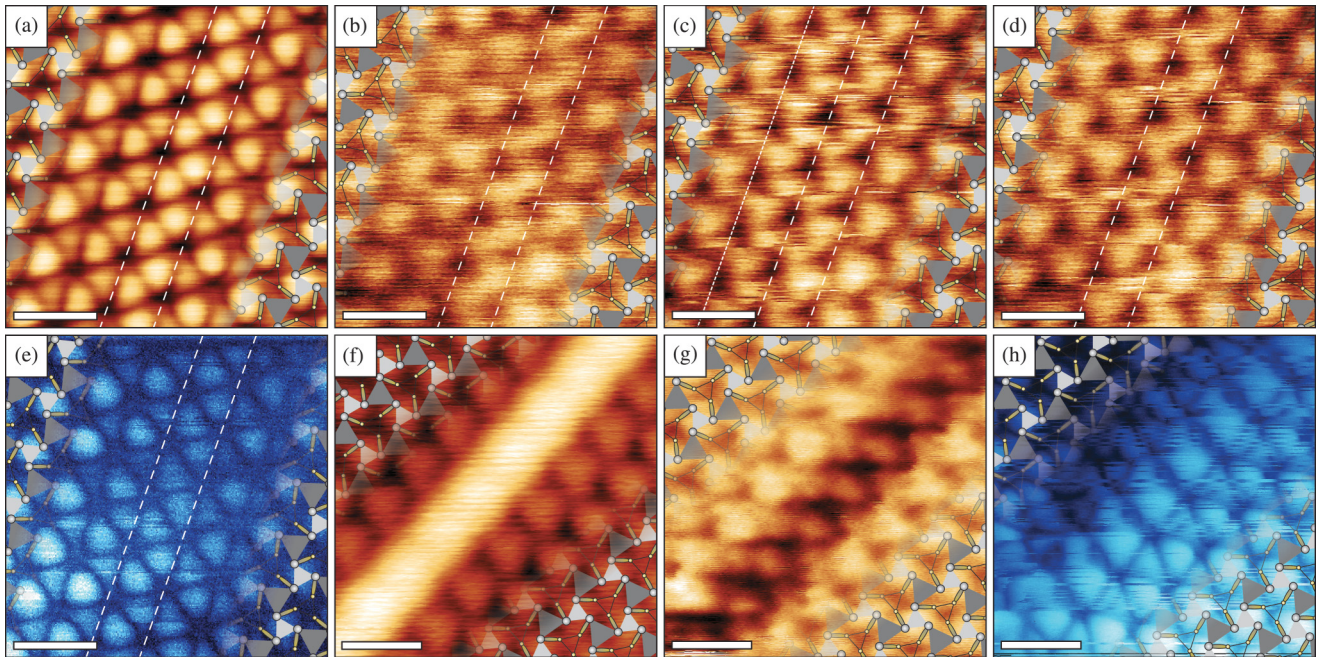
FIG. 4. (Color online) SPM images, taken at 5 K, showing (a)–(e) a chiral phase boundary (with the HCT row highlighted) and (f)–(h) a out-of-phase (with respect to the silicon trimers) boundary. In both cases, the IETa model is overlaid in the bottom right and the IETb model is overlaid in the top left. (a) dSTM topograph displaying inequivalent-trimer contrast ($V_{gap} = +1$ V, $\langle I_t \rangle = 100$ pA). (b)–(d) NC-AFM topographs displaying small-trimer contrast obtained with $\Delta f = -14.0, -14.9, -15.4$ Hz, respectively. (e) Tunnel current image corresponding to (d) ($V_{gap} = +400$ mV, $\langle I_t \rangle_{max} \simeq 5$ pA). (f) dSTM topograph displaying small-trimer contrast ($V_{gap} = +1$ V, $\langle I_t \rangle = 200$ pA). (g) Subsequent NC-AFM topograph also displaying small-trimer contrast and (h) corresponding tunnel current image ($\Delta f = -9$ Hz, $V_{gap} = 50$ mV, $\langle I_t \rangle_{max} \simeq 50$ pA). Note that FFT filtering has been applied to (g) to remove mechanical noise. All images acquired with $a = 0.2$ nm, all scale bars are 1 nm.

described by an IET configuration (IETb in our case) and are located at the vertices of the triangles shown in Fig. 3(b). In Fig. 3(d), the positions of tunnel current maxima are centered on Ag trimers as determined from the NC-AFM image, however, these triangles are rotated ~40° relative to those in Fig. 3(b) (where agreement with the model is astonishingly good), but no change in the surface has taken place. Consequently, the direction of triangles in STM imaging can clearly be dominated by the symmetry of the tip apex and does not necessarily represent the actual orientation of Ag trimers. We note in passing that a small gradient is apparent on the tunnel current images, most likely due to a nearby surface defect or subsurface dopant resulting in local band bending. However, in the absence of a larger scan showing the origin of the gradient, a definitive statement regarding its origin is difficult. However, we have observed similar features on clean silicon surfaces and note that these features are often not easily observable at higher bias, which is consistent with reported conventional STM imaging of charged defects on related surfaces.

The imaging of Ag atoms with NC-AFM at low temperature provides two key pieces of information. First, that NC-AFM is capable of resolving the IET configuration, as theoretically predicted. Second, it demonstrates that NC-AFM is able to resolve, uniquely, the absolute chirality of the surface (i.e., IETa or IETb). Although previous studies have been able to detect regions of differing chirality, only the relative chirality could be inferred.[11]

It is known that the stability of Ag trimers of the Ag:Si(111) surface can be influenced by the presence of defects and step

edges in the local environment.[12,26] Consequently, here it is demonstrated that the surface can be imaged stably in NC-AFM even at an unstable chiral boundary, i.e., a boundary between IETa and IETb chiral configurations. By comparing a dSTM image to an NC-AFM image of the same region, see Figs. 4(a) and 4(b), respectively, it can be shown that the triangles in NC-AFM correspond to the small Ag trimers in dSTM (imaged as bright and large). It should be noted that fundamentally this is the same imaging mode as shown in Fig. 3(c), but the atomic positions are not as clearly resolved. Whether the Ag atoms are clearly resolved likely depends on both the exact bonding of the tip terminating atom, and the imaging set point (cf. Fig. 5 of Ref. 23).

At the phase boundary, it is thought that small regions of the true HCT configuration exist (though the width of such regions remains uncertain).[20] The NC-AFM image in this instance confirms that the highlighted row of trimers is forced into the HCT configuration. At high set points, there is evidence that the physical interaction with the tip causes surface modification along the phase boundary, see Fig. 4(c) where an additional line (with smaller dashes) has been added to indicate the row under perturbation. This effect has previously been noted in STM experiments,[12,27] but the manipulation mechanism is not well defined. Although tunnel-current-based manipulation may play a role in STM, these images suggest that direct physical tip-sample interactions could also play a crucial role as no tunnel current was detected during the scan showing manipulation.[33] We note, however, that in this instance, no permanent change of the phase

boundary was observed, i.e., it appears each manipulation was subsequently reversed. We also detected no atomic scale contrast in the dissipation signal during this scan[33] suggesting that the manipulation did not occur during every oscillation cycle. In the absence of controlled single trimer manipulation data, it is difficult to make any specific comment about the exact nature of the manipulation mechanism. In Fig. 4(d), a small bias is applied to the tip; the corresponding tunnel current image confirms the assignment of the NC-AFM contrast and shows a strong similarity to the dSTM image, see Fig. 4(e) cf. Fig. 4(a).

For comparative purposes a stable out-of-phase boundary, i.e., a boundary due to registration mismatch of Si trimers on the Si(111) unreconstructed surface,[28] was also imaged. Figures 4(f)–4(h) show this boundary images as a protrusion in dSTM and a depression in NC-AFM. The accepted model for this boundary has a missing row of silicon trimers, and the depression in this region reflects an absence of Ag and Si at this position. Although a less reactive region of the same topographic height would produce a similar effect, we suggest that given the unreactive nature of the Ag surface, and the confirmation to the accepted model, it seems likely that in this instance, the apparent topographic depression is caused by the topography, and not by a change in reactivity of the surface. Again, the topographic maxima in NC-AFM correspond to the small Ag trimers. Coincidently, Figs. 4(f)–4(h) display a boundary between IETa and IETb regions, however, a change in chirality across this boundary type is not required.

Comparing the imaging of the IET configuration at 5 K with previous simulated NC-AFM of the surface at 0 K,[23] we see a very strong similarity with simulated images acquired with a Si-terminated tip. On this basis we suggest that the initial assignment of Ag-atom contrast to an Ag-terminated tip, and Ag-Si-bond contrast to an Si-terminated tip[14,15] may need to be re-evaluated. We also note there is considerable variation in the maxima positions between different images and tips; in some cases, the maxima are located very close to the Si atom position itself, whereas in other cases, the maxima is more closely aligned to the Ag-Si bond position. Conclusively, resolving the assignment of the tip termination for each imaging mode and the location of the interaction maxima in the "Ag-Si bond/Si atom" imaging mode might be accomplished by further simulated imaging with an Ag-terminated tip.

C. Imaging at an intermediate temperature (77 K)

Figure 5 shows images of the Ag:Si(111) surface acquired by NC-AFM, with a small applied bias, at 77 K. At low set points, triskelions (shapes with three protrusions and threefold rotational symmetry), as previously reported by Minobe *et al.*,[15] are observed, see Fig. 5(a). As the frequency shift set point is increased, these triskelions "close up" to form triplets of topographic maxima corresponding to Ag-Si bonds, see Figs. 5(a), 5(c), and 5(e). This confirms that the same set-point-dependent transition previously reported at room temperature also occurs at lower temperatures. Unexpectedly, although the tunnel current displays an IET appearance, the topography appears to be closer to an HCT appearance. An image acquired at the same temperature with a tip showing topographic maxima over Ag atoms also displays an HCT
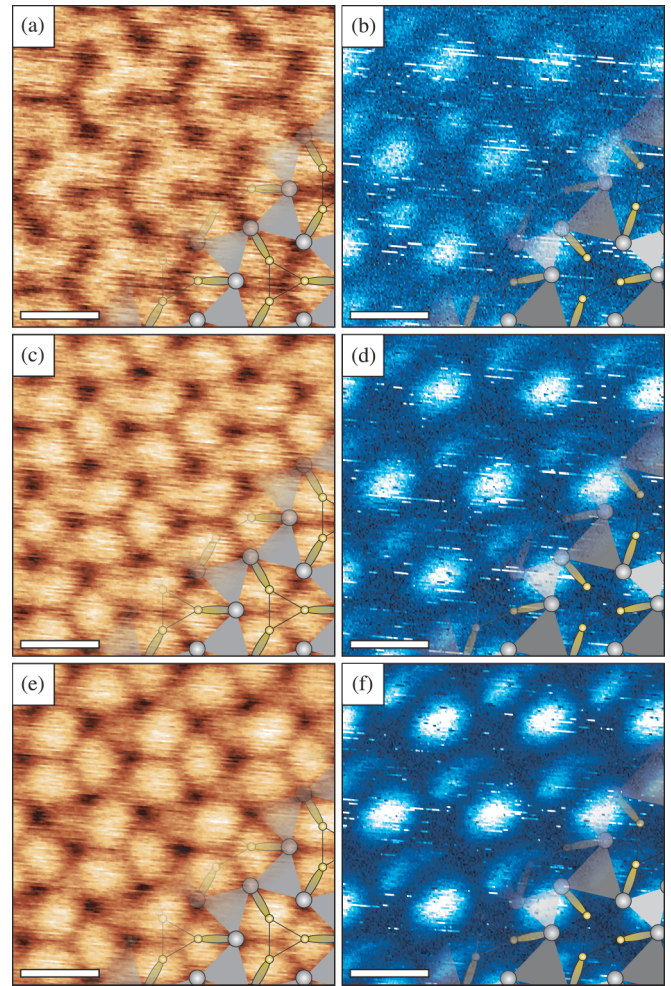
FIG. 5. (Color online) Topographic NC-AFM and simultaneously acquired tunnel current images, taken at 77 K, showing set-point-dependent contrast variation. The HCT model is overlaid on topographies, whilst the IETa model is overlaid on tunnel current images. (a) Topograph and (b) tunnel current image at low set point ($\Delta f = -11.9$ Hz, $\langle I_t \rangle_{\max} \simeq 26$ pA). (c) Topograph and (d) tunnel current image at an intermediate set point ($\Delta f = -13.0$ Hz, $\langle I_t \rangle_{\max} \simeq 44$ pA). (e) Topograph and (f) tunnel current image at a high set point ($\Delta f = -13.7$ Hz, $\langle I_t \rangle_{\max} \simeq 58$ pA). See Supplemental Material for the corresponding zero-bias images and drift correction. Images acquired with $a = 0.2$ nm and $V_{\mathrm{gap}} = +1$ V, all scale bars are 0.5 nm.

appearance, see Fig. 6. These observations must be balanced with STM data acquired in the same area displaying an IET appearance and a chiral phase boundary which cannot be explained by the presence of a tip artefact, see Supplemental Material. However, other images acquired with the Ag-Si-bond contrast seem to be closer to an IET appearance, see Fig. 7, with the tunnel current confirming this assignment. Therefore, at 77 K, the surface clearly adopts an IET configuration, and an obvious question arises: why is an HCT appearance sometimes observed in NC-AFM when an IET configuration is seen in the simultaneously acquired tunnel current?

Importantly, we note that even the interpretation of STM images of Ag:Si(111) at 77 K can be nontrivial. Normally, STM contrast related to the Ag atom positions is only acquired
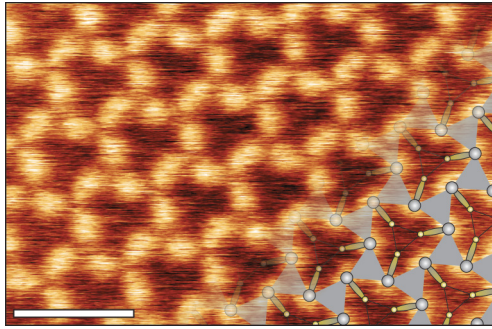
FIG. 6. (Color online) NC-AFM topograph, taken at 77 K, displaying Ag-atom contrast, with the HCT model overlaid ($\Delta f = -14.8$ Hz, $a = 0.2$ nm, $V_{gap} \simeq 0$ V). 1 nm scale bar.

with negative sample biases,[29] however, in Fig. 8, we show that (with a particular tip state) we can observe the Ag atom positions with positive bias. Intriguingly, at higher bias, the IET configuration with small-trimer contrast is observed, whereas it appears it that the Ag atom positions relate more closely to an HCT appearance. Comparison to simultaneous NC-AFM/STM imaging conducted at negative bias at 5 K shows an IET configuration is resolvable at low temperature in the tunnel current, see Fig. 9.

In order to understand the difference in image contrast between NC-AFM and STM, attention must be paid to three critical factors: the energy barriers between the two IET chiral configurations (with and without the presence of the tip); the amount of thermal energy available at 5, 77, and
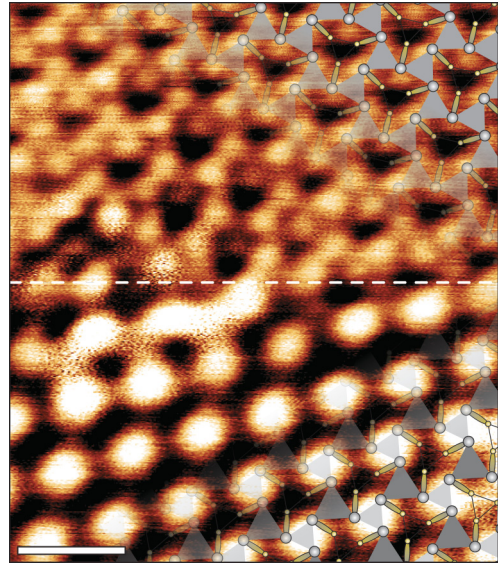
FIG. 8. (Color online) Topographic STM image, taken at 77 K, with V_{gap} changed between $+2$ V (lower, IETa model overlaid) to $+1.5$ V (upper, HCT model overlaid). $I_t = 100$ pA, 1 nm scale bar.

300 K; and the state of the surface, and its relative influence on the frequency shift and tunnel current channels, over an oscillation cycle of the cantilever. First, it has been shown that the position of the tip affects the relative stability of the IETa and IETb configurations, and this statistical weighting, coupled with thermal effects, explains the observed HCT appearance at room temperature.[23] Second, the amount of thermal energy available at 77 K is significantly reduced compared to 300 K, but on the related Si(100) surface, it has been shown that this can still provide sufficient energy to cause the surface to relax from a tip perturbed state on, or faster than, the time scale of a cantilever oscillation.[18] Assuming an energy barrier between the two IET configurations of $\Delta E \simeq 100$ meV,[13] a prefactor $\upsilon_0 \simeq 10^{12}$ Hz, and the relationship $\upsilon = \upsilon_0 e^{-\Delta E/k_B T}$, at 300 K trimers should oscillate between the two configurations at $\upsilon \simeq 2 \times 10^{10}$ Hz, whilst at 5 K there is no oscillation ($\upsilon \simeq 1 \times 10^{-89}$ Hz). However, at 77 K, the flipping rate is $\upsilon \simeq 3 \times 10^5$ Hz, comparable to the cantilever oscillation frequency on resonance $f_0 \simeq 2 \times 10^4$ Hz. We note that this simple calculation does not take into account the perturbation of the energy barrier due to the presence of the tip (which itself will be tip-position-dependent
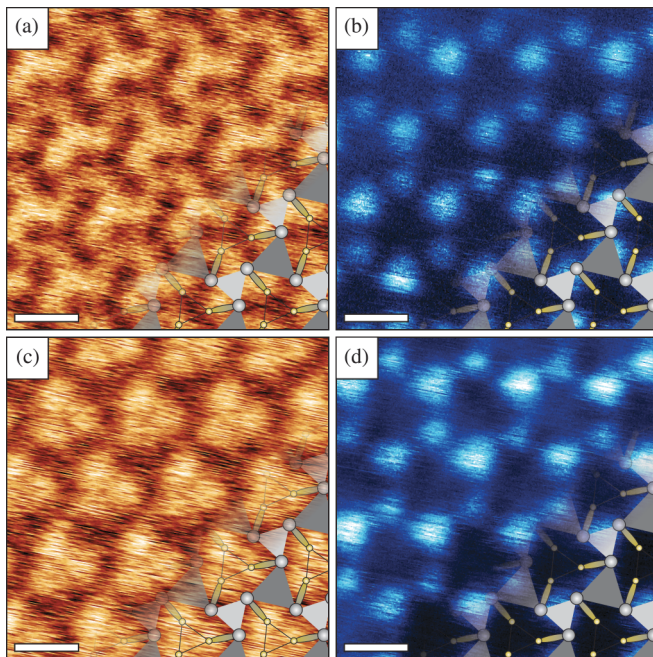
FIG. 7. (Color online) Topographic NC-AFM and simultaneously acquired tunnel current images, taken at 77 K, with a different tip apex compared to Fig. 5, with IETa model overlaid. (a) Topograph and (b) tunnel current image at low set point ($\Delta f = -11$ Hz, $\langle I_t \rangle_{max} \simeq 25$ pA). (c) Topograph and (d) tunnel current image at high set point ($\Delta f = -16$ Hz, $\langle I_t \rangle_{max} \simeq 40$ pA). Images acquired with $a = 0.2$ nm and $V_{gap} = +600$ mV. All scale bars are 0.5 nm.
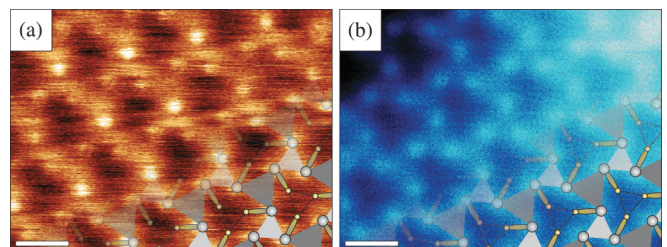
FIG. 9. (Color online) (a) Topographic NC-AFM and (b) simultaneously acquired tunnel current images, taken at 5 K, displaying Ag-atom contrast, with IETb model overlaid ($\Delta f = -69$ Hz, $a = 0.2$ nm, $V_{gap} = -200$ mV, $\langle I_t \rangle_{max} \simeq 20$ pA). 0.5 nm scale bars.

and vary over an oscillation cycle) nor the possible variation in energy barrier due to defects or adsorbates in the locality of a trimer.

Third, understanding how the short-range chemical force and tunnel current integrate over the oscillation cycle for a dynamically fluctuating surface is nontrivial. Although both chemical force and tunnel current are strongly weighted towards the point of closest approach of the oscillation, it has been shown that the tunnel current signal typically shows atomic contrast several angstroms above the point at which the chemical forces become detectable.[25] Therefore it may be possible that the tunnel current signal is weighted such that the imaging arises from a point in the oscillation cycle where the surface remains unperturbed. The NC-AFM topography contrast should only arise from the very closest point of approach, and will therefore be dominated by the state of the surface at the moment of strongest tip-sample interaction. A similar effect has been observed in experiments on the Si(100) surface at 77 K, where in some cases the buckled $c(4 \times 2)$ ground state was observed in the tunnel current image, whereas the tip induced $p(2 \times 1)$ periodicity was observed in the topography.[30] Moreover, depending on the balance of the energy barriers, a "mixed state" between the IET and HCT configurations could be observed, again similar to that proposed for the Si(100) surface.[18,30] This will have a critical dependence on both the chemical reactivity of the tip apex, and the electronic density of states, and this may explain the apparent variation between the HCT and IET appearances observed in the topographs during NC-AFM imaging at 77 K. Regardless, a complete understanding of the relative contributions to the chemical force and tunnel current during approach and retract, at intermediate temperatures, on a unstable surface, will require a considerable theoretical undertaking in its own right, and is beyond the scope of this experimental investigation.

In comparing the data acquired at cryogenic temperatures and room temperature, it is important to address the difference in the magnitude of the detected tunnel current signal and the relative degree of perturbation between the two setups. Importantly, in the low-temperature experiments, the gap voltage was tuned to ensure a small, but detectable, tunnel current signal in order to avoid cross-talk effects,[33] often increasing the gap voltage even a few hundred meV could result in tunnel current signals several orders of magnitude larger. In the room-temperature experiments, the gap voltage was set to ensure good topographic and tunnel current imaging, often resulting in significant tunnel currents. However, the magnitude of the tunnel current detected at a given bias is strongly tip dependent, and the magnitude of the tunnel current at closest approach is likely to have been much larger in the room temperature case as the large oscillation amplitude results in the tip spending a much larger proportion of the oscillation cycle out of tunneling (for a given detected average tunnel current). However, since the atomic scale contrast in the frequency shift signal is dominated by the onset of chemical bonding between tip and sample at the point of closest approach, it seems likely that the point of closest approach at both room and cryogenic temperatures is broadly comparable. In addition, since we do not observe any qualitative difference in imaging either with, or without, tunnel current, it does not seem that tunneling electrons are responsible for any additional detectable perturbation in these experiments. Consequently, although it is difficult to make a quantitative comparison in the point of closest approach between the room-temperature and low-temperature experiments from imaging alone (and, indeed, even between different tips at the same temperature), it seems unlikely that the HCT appearance at room temperature is caused by additional perturbation of the surface due to a closer approach resulting from the larger oscillation amplitudes.

IV. CONCLUSIONS

In conclusion, we have used simultaneous NC-AFM/STM to resolve controversy surrounding the interpretation of NC-AFM imaging of the Ag:Si(111) surface. We observe tunnel current maxima over the center of the Ag trimers (regardless of the contrast in NC-AFM), have shown that NC-AFM can resolve the Ag atom positions in an IET configuration at 5 K, and can determine the absolute chirality of the surface. A thermally averaged HCT appearance is observed at room temperature in both NC-AFM and STM. At intermediate temperatures, the delicate balance of the energy barriers between the two IET chiral configurations during the close approach of the tip and the available thermal energy of the system can result in an HCT appearance in NC-AFM, whereas the simultaneously acquired tunnel current data show an unperturbed IET configuration. Future investigations will focus on combining this technique with density functional theory (DFT) simulations in order to determine the tip structures that result in the observed contrasts, and the effect of thermal fluctuations on the frequency shift and averaged tunnel current signals.

[1] S. Watanabe, M. Aono, and M. Tsukada, Phys. Rev. B **44**, 8330 (1991).

[2] E. J. van Loenen, J. E. Demuth, R. M. Tromp, and R. J. Hamers, Phys. Rev. Lett. **58**, 373 (1987).

[3] R. J. Wilson and S. Chiang, Phys. Rev. Lett. **58**, 369 (1987).

[4] R. J. Wilson and S. Chiang, Phys. Rev. Lett. **59**, 2329 (1987).

[5] J. E. Demuth, E. J. von Lenen, R. M. Tromp, and R. J. Hamers, J. Vac. Sci. Technol. B **6**, 18 (1988).

[6] Y. G. Ding, C. T. Chan, and K. M. Ho, Phys. Rev. Lett. **67**, 1454 (1991).

[7] S. Watanabe, M. Aono, and M. Tsukada, Jpn. J. Appl. Phys. **32**, 2911 (1993).

[8] S. Watanabe, M. Aono, and M. Tsukada, Surf. Sci. **287**, 1036 (1993).

[9] H. M. Zhang, J. B. Gustafsson, and L. S. O. Johansson, Phys. Rev. B **74**, 201304(R) (2006).

[10] H. M. Zhang, J. B. Gustafsson, and L. S. O. Johansson, J. Phys.: Conf. Ser. **61**, 1336 (2007).

[11] H. Aizawa, M. Tsukada, N. Sato, and S. Hasegawa, Surf. Sci. **429**, L509 (1999).

[12] N. Sato, T. Nagao, and S. Hasegawa, Surf. Sci. **429**, 65 (1999).

[13] N. Sasaki, S. Watanabe, H. Aizawa, and M. Tsukada, Surf. Sci. **493**, 188 (2001).

[14] K. Yokoyama, T. Ochi, Y. Sugawara, and S. Morita, Phys. Rev. Lett. **83**, 5023 (1999).

[15] T. Minobe, T. Uchihashi, T. Tsukamoto, S. Orisaka, Y. Sugawara, and S. Morita, Appl. Surf. Sci. **140**, 298 (1999).

[16] K. Hata, Y. Sainoo, and H. Shigekawa, Phys. Rev. Lett. **86**, 3084 (2001).

[17] Y. Pennec, M. HornvonHoegen, X. Zhu, D. C. Fortin, and M. R. Freeman, Phys. Rev. Lett. **96**, 026102 (2006).

[18] L. Kantorovich and C. Hobbs, Phys. Rev. B **73**, 245420 (2006).

[19] S. Watanabe, Y. Kondo, Y. Nakamura, and J. Nakamura, Sci. Technol. Adv. Mater. **1**, 167 (2000).

[20] Y. Nakamura, Y. Kondo, J. Nakamura, and S. Watanabe, Phys. Rev. Lett. **87**, 156102 (2001).

[21] N. Sasaki, H. Aizawa, and M. Tsukada, Appl. Surf. Sci. **157**, 367 (2000).

[22] K. Kakitani, A. Yoshimori, H. Aizawa, and M. Tsukada, Surf. Sci. **493**, 200 (2001).

[23] N. Sasaki, S. Watanabe, and M. Tsukada, Phys. Rev. Lett. **88**, 046106 (2002).

[24] F. J. Giessibl, Appl. Phys. Lett. **76**, 1470 (2000).

[25] Y. Sugimoto, Y. Nakajima, D. Sawada, K. I. Morita, M. Abe, and S. Morita, Phys. Rev. B **81**, 245322 (2010).

[26] Y. Nakamura, H. Koga, and S. Watanabe, J. Phys. Soc. Jpn. **72**, 13 (2003).

[27] B. Li, C.-G. Zeng, H.-Q. Wang, B. Wang, and J.-G. Hou, Chin. Phys. Lett. **18**, 181 (2001).

[28] D. W. McComb, R. A. Wolkow, and P. A. Hackett, Phys. Rev. B **50**, 18268 (1994).

[29] K. J. Wan, X. F. Lin, and J. Nogami, Phys. Rev. B **45**, 9509 (1992).

[30] A. Sweetman, R. Danza, S. Gangopadhyay, and P. Moriarty, J. Phys.: Condens. Matter **24**, 084009 (2012).

[31] A. Sweetman, S. Jarvis, R. Danza, J. Bamidele, S. Gangopadhyay, G. A. Shaw, L. Kantorovich, and P. Moriarty, Phys. Rev. Lett. **106**, 136101 (2011).

[32] H. Tajiri, K. Sumitani, S. Nakatani, A. Nojima, T. Takahashi, K. Akimoto, H. Sugiyama, X. Zhang, and H. Kawata, Phys. Rev. B **68**, 035330 (2003).

[33] See Supplemental Material at http://link.aps.org/supplemental/10.1103/PhysRevB.87.075310 for additional information on the experimental setup and additional experimental data.